World Journal of Gastroenterology

Online Submissions: http://www.wjgnet.com/esps/
wjg@wjgnet.com
doi:10.3748/wjg.v18.i35.4967

World J Gastroenterol 2012 September 21; 18(35): 4967-4972
ISSN 1007-9327 (print) ISSN 2219-2840 (online)

CASE REPORT

Hepatic schwannoma: Imaging findings on CT, MRI and contrast-enhanced ultrasonography

Yu Ota, Kazunobu Aso, Kenji Watanabe, Takahiro Einama, Koji Imai, Hidenori Karasaki, Ryuji Sudo, Yosui Tamaki, Mituyoshi Okada, Yosihiko Tokusashi, Toru Kono, Naoyuki Miyokawa, Masakazu Haneda, Masahiko Taniguchi, Hiroyuki Furukawa

Yu Ota, Kazunobu Aso, Ryuji Sudo, Yosui Tamaki, Mituyoshi Okada, Masakazu Haneda, Division of Metabolism and Biosystemic Science, Department of Medicine, Asahikawa Medical University, Asahikawa 078-8510, Japan
Kenji Watanabe, Takahiro Einama, Koji Imai, Hidenori Karasaki, Toru Kono, Masahiko Taniguchi, Hiroyuki Furukawa, Division of Gastroenterologic and General Surgery, Department of Surgery, Asahikawa Medical University, Asahikawa 078-8510, Japan
Yosihiko Tokusashi, Naoyuki Miyokawa, Department of Pathology, Asahikawa Medical University, Asahikawa 078-8510, Japan
Author contributions: Ota Y contributed to this work mainly; Ota Y, Aso K, Watanabe K, Einama T, Imai K, Karasaki H, Sudo R, Tamaki Y, Okada M, Kono T, Haneda M, Taniguchi M and Furukawa H provided medical care; Ota Y, Aso K and Taniguchi M collected the images; Tokusashi Y and Miyokawa N diagnosed the patient pathologically; Ota Y and Taniguchi M wrote the paper.
Correspondence to: Masahiko Taniguchi, MD, Division of Gastroenterologic and General Surgery, Department of Surgery, Asahikawa Medical University, Asahikawa 078-8510, Japan. m-tani@asahikawa-med.ac.jp
Telephone: +81-166-682503 Fax: +81-166-682193
Received: February 29, 2012 Revised: May 12, 2012
Accepted: May 26, 2012
Published online: September 21, 2012

Abstract

A primary benign schwannoma of the liver is extremely rare and is difficult to preoperatively discriminate from a malignant tumor. We compared the imaging and pathological findings, and examined the possibility of preoperatively diagnosing a benign liver schwannoma. A 72-year-old woman was admitted to our hospital because of a 4.6-cm mass in the liver. A malignant tumor was suspected, and a right hepatectomy was performed. After this, the diagnosis of a primary benign schwannoma of the liver was made through pathological examination. Contrast-enhanced ultrasonography (CEUS) with Sonazoid showed minute blood flows into the septum and solid areas of the tumor in the vascular phase; most likely due to increased arterial flow associated with infiltration of chronic inflammatory cells. In the postvascular phase, CEUS showed contrast defect of cystic areas and delayed enhancement of solid areas; most likely due to aggregation of siderophores. Because discriminating between a benign and malignant schwannoma of the liver is difficult, surgery is generally recommended. However, the two key findings from CEUS may be useful in discriminating ancient schwannoma by recognizing the hemorrhage involved in the secondary degeneration and aggregation of siderophores.

Key words: Liver schwannoma; Contrast-enhanced ultrasonography; Liver resection

Peer reviewers: Dr. Avinash R Kambadakone, Division of Abdominal Imaging and Intervention, Department of Radiology, Massachusetts General Hospital, White 270, 55 Fruit Street, Boston, MA 02114, United States; Luis Bujanda, Professor, Donostia Hospital, Avda. Sancho El Sabio 17-2Dcha, 20010 San Sebastián, Spain

Ota Y, Aso K, Watanabe K, Einama T, Imai K, Karasaki H, Sudo R, Tamaki Y, Okada M, Tokusashi Y, Kono T, Miyokawa N, Haneda M, Taniguchi M, Furukawa H. Hepatic schwannoma: Imaging findings on CT, MRI and contrast-enhanced ultrasonography. *World J Gastroenterol* 2012; 18(35): 4967-4972 Available from: URL: http://www.wjgnet.com/1007-9327/full/v18/i35/4967.htm DOI: http://dx.doi.org/10.3748/wjg.v18.i35.4967

INTRODUCTION

A schwannoma is a benign nerve sheath tumor that

originates from the Schwann cells of the nerve sheath. Schwannomas can occur in patients at any age, but are most commonly detected in patients between 20 years and 50 years of age. Although a schwannoma can develop in any part of the body, the most common sites include the head, neck, and flexor surfaces of the extremities[1]. Schwannomas develop infrequently in the gastrointestinal tract, the retroperitoneal cavity, and any other part of the body[2]. Thus, a primary benign schwannoma of the liver is extremely rare. Preoperative discrimination between a benign and malignant schwannoma is difficult; therefore, operation is typically recommended for a diagnosis. In the current study, we used a combination of computed tomography (CT), magnetic resonance imaging (MRI), and positron emission tomography (PET), but discrimination was still difficult. The use of preoperative imaging findings to detect liver schwannoma or the use of contrast-enhanced ultrasonography (CEUS) to detect and characterize focal liver lesions has not been previously undertaken. In this paper, we report a case of benign schwannoma, which we diagnosed using a novel method that combined CEUS with CT, MRI and PET imaging. In addition, we compared the imaging and pathological findings.

CASE REPORT

A 72-year-old woman was admitted to our hospital because a 4.6-cm mass was detected in her liver by ultrasonography (US) at a private clinic. Upon physical examination, the abdomen was soft and flat without tenderness. The liver, spleen, and superficial lymph nodes were not palpable. Blood analysis showed almost normal liver function. Carcinoembryonic antigen (CEA) and α-fetoprotein (AFP) were both negative. Hepatitis B surface antigen and hepatitis B e antibody were positive, but hepatitis C virus marker was negative. The patient's serum antibodies were negative for specific echinococcal antigens.

CT, MRI, PET and CEUS were used for the qualitative diagnosis of the liver mass. Multiphasic contrast-enhanced CT in the arterial dominant, portal venous and late venous phases was performed using a 64-slice CT scanner. A CT scan of the abdomen showed an approximately 5-cm, well-defined round tumor in segment 8 of the right hepatic lobe. The mass was hypodense and contained a minute partial calcification (Figure 1A). The mass showed heterogeneous enhancement in the arterial dominant phase (Figure 1B) and delayed enhancement until the portal venous (Figure 1C) and late venous (Figure 1D) phases. There was no evidence of fatty infiltration or cirrhosis in the background liver.

MRI revealed a hypointense mass with T1-weighted imaging (Figure 2A) and a mixed hypo- and hyperintense mass with T2-weighted imaging (Figure 2B) and diffusion-weighted imaging (DWI) (Figure 2C). The diffusion images were obtained with a b value of 1000 s/mm^2. Because the mass was hyperintense on the apparent diffusion coefficient maps, it was also hyperintense on DWI under the influence of the T2 shine-through. Gadolinium-ethoxybenzyl-diethylenetriamine penta-acetic acid (Gd-EOB-DTPA) was injected at 0.025 mmol/kg body weight. Gd-EOB-DTPA-enhanced MRI showed heterogeneous enhancement in the arterial phase and delayed enhancement until the late venous phase (similar to dynamic CT imaging), but a defect in the hepatobiliary phase (Figure 2D).

An F-18 fluorodeoxyglucose PET (FDG-PET) system was used (Discovery VCT; GE Healthcare, Tokyo, Japan) with the following conditions: PET, 2-3 min/1 bed, 3.75-mm slice; CT, 120 kV, 100 mA with auto mA; tube rotation time, 0.6 s/rotation; detector collimation, 64 mm × 1.25 mm; beam pitch, 0.984; section thickness, 5.0 mm; and reconstruction pitch, 3.27 mm. FDG-PET revealed abnormal uptake in the lesion, with a maximum standardized uptake value of 3.9. There was no additional lesion in the liver, no evidence of extrahepatic disease, and no lymphadenopathy.

US showed a 4.6-cm mass that contained multiple hypoechoic cysts with mixed internal septations and solid areas (Figure 3A). CEUS with Sonazoid showed minute blood flows into the septum and solid areas of the tumor in the vascular phase (Figure 3B), and contrast defects of cystic areas and delayed enhancement of solid areas in the postvascular phase (Figure 3C).

A malignant tumor, such as a biliary cystadenocarcinoma or cholangiocellular carcinoma (CCC), was suspected. Because there was danger of seeding, we did not perform a biopsy. An operation was performed to remove the mass. At surgery, it was discovered that the tumor originated from the anterior segment of Glisson's sheath, but was tightly attached to the posterior segment of the sheath. Intraoperative cholangiography revealed a stricture in the posterior segment of the bile duct, and there was no extension of the distal bile duct. The bile duct did not have a tumor projection until strangulation. Because the tumor involved the bile duct, dissection was not possible; therefore, the patient underwent right hepatectomy.

The gross findings were a well-circumscribed, whitish/brownish, localized mass, 4.5 cm in size, which was surrounded by a fibrous capsule. The division surface of the tumor showed large and small multilocular cysts. Microscopic examination revealed that the tumor was adjacent to the peripheral nerve of the portal area, and the Antoni A hypercellular area and Antoni B hypocellular area were present in a complex (Figure 4A). In the Antoni A region, an array of irregular groups of spindle cells was seen, but nuclear palisading with Verocay bodies was not observed. In the Antoni B region, there was edematous stroma, vasodilatation, aggregation of siderophores, and slight permeation of chronic inflammatory cells of the histiocyte and the lymphocyte types (Figure 4B). Immunohistochemical staining showed a strong positive S-100 protein reaction. Vimentin, nonspecific enolase, bcl-2, and MIC2 (also known as CD99) staining

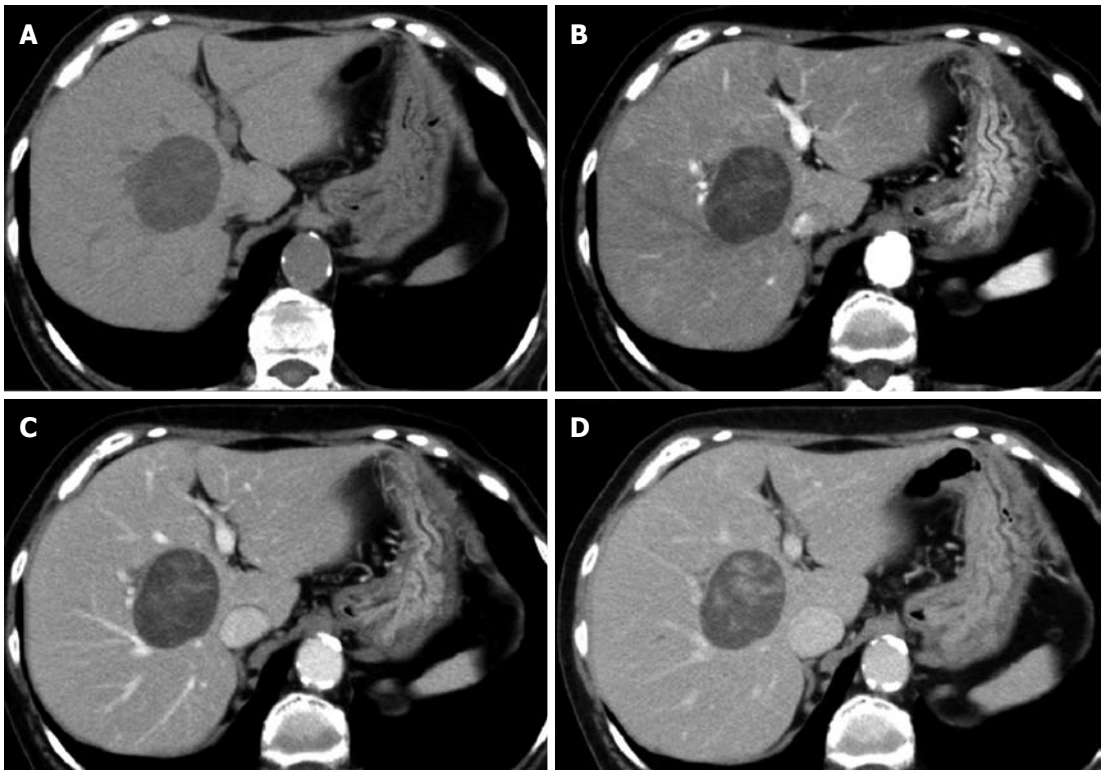

Figure 1 Abdominal computed tomography. A: Plain; B: Arterial dominant phase; C: Portal venous phase; D: Late venous phase. Abdominal computed tomography (CT) showed an approximately 5-cm well-defined round tumor in segment 8 of the right hepatic lobe. CT showed heterogeneous enhancement in the arterial dominant phase; and delayed the enhancement until the portal venous and late venous phases.

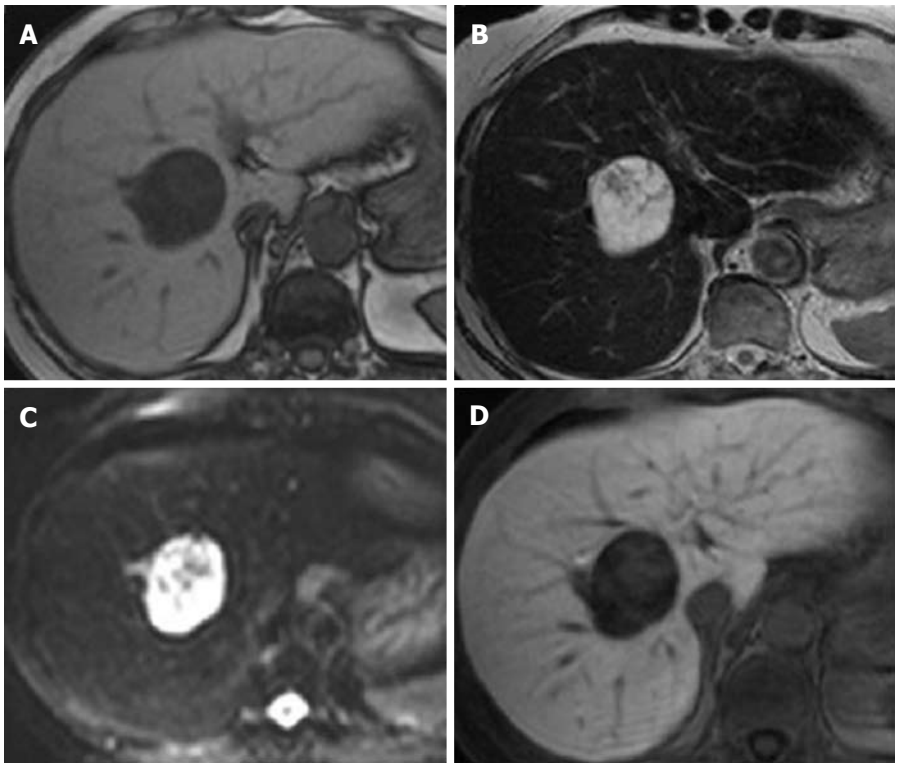

Figure 2 Magnetic resonance imaging. A: T1-weighted imaging; B: T2-weighted imaging; C: Diffusion-weighted imaging (DWI); D: Hepatobiliary phase. Magnetic resonance imaging (MRI) revealed a hypointense mass on T1-weighted imaging, and a mixed hypo- and hyperintense mass on T2-weighted imaging and on DWI. Gadolinium-ethoxybenzyl-diethylenetriamine penta-acetic acid-enhanced MRI showed a defect in the hepatobiliary phase.

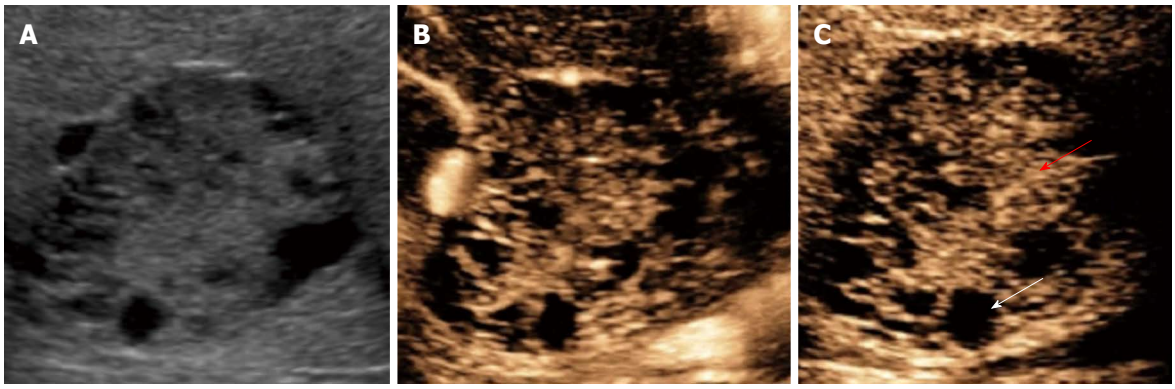

Figure 3 Contrast-enhanced ultrasonography with Sonazoid. A: B-mode ultrasound; B: Vascular phase; C: Postvascular phase. Ultrasonography showed a 4.6-cm mass that contained multiple hypoechoic cysts with mixed internal septations and solid areas. Contrast-enhanced ultrasonography with Sonazoid showed minute blood flow into the septum and solid areas of the tumor in the vascular phase, and contrast defect of cystic areas (white arrow) and delayed enhancement of solid areas (red arrow) in the postvascular phase.

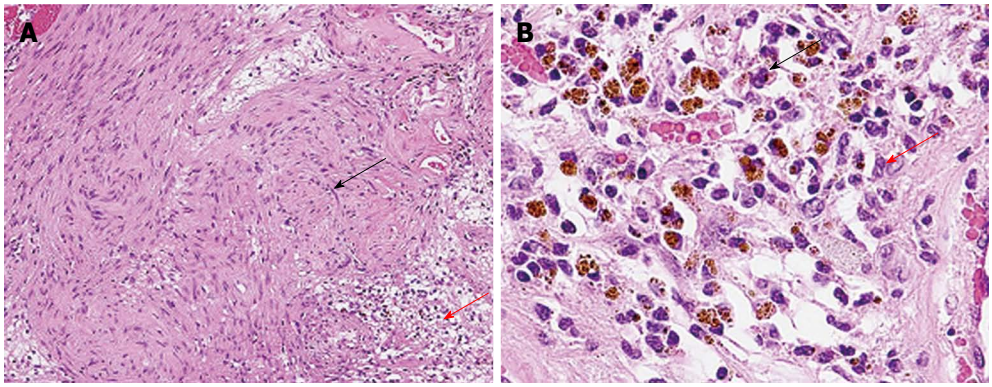

Figure 4 Microscopic examination. A: B-mode ultrasound. Microscopic examination revealed that Antoni A hypercellular area (black arrow) and Antoni B hypocellular area (red arrow) existed together in a complex; B: Vascular phase. In the Antoni B region, there were edematous stroma, vasodilatation, aggregation of siderophores (black arrow), and slight permeation of chronic inflammatory cells of the histiocyte and lymphocyte types (red arrow).

was also positive. The MIB-1 index was 2%. However, desmin, α-smooth muscle actin, CD34, c-kit, HMB-45, neurofilament, glial fibrillary acidic protein, and cytokeratin (AE1/AE3) staining was all negative.

On the basis of these findings, we diagnosed the patient as having a primary benign schwannoma of the liver. The patient was healthy and free from recurrence at a follow-up CT scan, which was performed 12 mo after surgery.

DISCUSSION

Histologically, schwannomas are encapsulated tumors that arise within nerve sheaths and consist of a highly ordered cellular component (Antoni A area) and a loose myxoid component (Antoni B area). In the subcellular component, spindle cells are present. Larger schwannomas have a tendency to undergo secondary degeneration, such as pseudocystic regression, hemorrhage, and calcification[3]. A primary benign schwannoma of the liver is an isolated benign tumor surrounded by a fibrous capsule. Immunohistochemical staining is diffusely and strongly positive for S-100 protein in a schwannoma, which is consistent with the markers for a nerve sheath tumor[3]. There are no specific characteristics with regard to the radiological appearance[1].

We reviewed the country of origin, size, age, sex, associated diseases, diagnosis, and prognosis of primary benign or malignant schwannomas; the findings are shown in Table 1[3-18]. Primary benign or malignant schwannomas were found in 14 women and 4 men. The age of onset was from 35 years to 74 years, and the mean age of onset was 57.5 years. While 13 cases were Asian in origin, there were no race differences. Although many hepatic schwannomas were Asian in origin, there has been no report of a causal relationship with hepatitis-associated viruses, and thus the reason for this correlation is unknown.

Generally, a CT scan depicts a schwannoma as a well-defined hypodense area, and enhanced CT shows peripheral enhancement, with an irregular pattern on the inside[10]. A delayed peripheral subject enhancement until the late venous phase in the CT scan reflects a fibrous capsule and an internal fibrillary element. With the aid of MRI, schwannomas have been described as masses with hypointensity on T1-weighted images and as masses with inhomogeneous hyperintensity or, in some cases, masses with internal heterogeneous mixed hypo- and hyperin-

Table 1 Review of primary benign or malignant schwannoma

Ref.	Age/sex	Country of origin	Size (cm)	Associated diseases	Diagnosis	Prognosis
Tuder *et al*[18]	74/M	North America	21 × 12 × 8	None	Surgery/autopsy	Death
Abe *et al*[17]	68/F	Asia	8.0 × 6.0 × 4.5	None	Surgery	Survival
Hytiroglou *et al*[16]	67/M	North America	13 × 11 × 10	None	-	-
Heffron *et al*[15]	38/F	North America	5	None	Surgery	Survival
Yoshida *et al*[14]	56/F	Asia	16	None	-	-
Morikawa *et al*[13]	63/M	Asia	20 × 13	None	Autopsy	Death
Sheikh *et al*[12]	35/F	Asia	-	None	-	-
Fiel *et al*[11]	49/M	North America	-	None	-	-
Wada *et al*[10]	69/F	Asia	15 × 13	None	Surgery	Survival
Wada *et al*[10]	64/F	Asia	4	Early gastric cancer	Surgery	Survival
Flemming *et al*[9]	57/F	Europa	Huge	None	Surgery	Survival
Momtahen *et al*[8]	52/F	Asia	4.4 × 3.6 × 2.9	None	Surgery	Survival
Lee *et al*[7]	36/F	Asia	5 × 4 × 2	None	Surgery	Survival
Akin *et al*[6]	66/F	Asia	3 × 5 × 4	Breast cancer	Biopsy/surgery	Survival
Shih *et al*[5]	58/F	Asia	9.1 × 7.1 × 8.9	None	Surgery	Survival
Sukegawa *et al*[4]	55/F	Asia	4.0 × 2.5 × 2.0	None	Surgery	Survival
Ozkan *et al*[3]	56/F	Asia	15 × 10 × 10	None	Surgery	Survival
Ota *et al* (present case)	72/F	Asia	4.6	None	Surgery	Survival

M: Male; F: Female.

Table 2 Comparison between preoperative imaging and pathological findings

Preoperative imaging technique		Characteristics	Pathology
Dynamic CT		Delayed peripheral subject enhancement	A fibrous capsule An internal fibrillary element
T2-weighted MRI		Internal heterogeneous mixed hypo- and hyperintensity	Secondary degeneration such as pseudocystic regression and hemorrhage
FDG-PET		Abnormal uptake	High cellular density (Antoni A area)
Ultrasonography	B mode	Mixed internal septations and solid areas	Division surface showed big and small multilocular cysts
	Vascular phase	Minute blood flows into septum and solid areas	Increased arterial vessel flows associated with infiltration of chronic inflammatory cells
	Postvascular phase	Delayed enhancement of solid areas	Aggregation of siderophores

CT: Computed tomography; MRI: Magnetic resonance imaging; FDG-PET: F-18 fluorodeoxyglucose-positron emission tomography.

tensity on T2-weighted images[8]. These findings reflect secondary degeneration, such as pseudocystic regression and hemorrhage. Abnormal uptake in FDG-PET reflects the high cellular density of schwannomas[19] (Table 2).

In this study, CT and MRI showed a tumor containing multiple cysts. Therefore, echinococcosis, hepatobiliary cystadenoma/adenocarcinoma or cystic liver metastasis of epithelial tumor, angiomyolipoma, leiomyoma, solitary fibrous tumor, schwannoma, or neurofibroma of the mesenchyma were possible differential diagnoses. However, it is very difficult to diagnose a schwannoma preoperatively based on its radiological appearance. Furthermore, abnormal uptake in FDG-PET did not aid the diagnosis.

Therefore, we used CEUS with Sonazoid for the preoperative diagnosis. Mixed internal septations and solid areas in B mode were reflected faithfully in the gross findings of a division surface with large and small multilocular cysts. CEUS showed minute blood flows into the septum and solid areas of the tumor in the vascular phase. The start of an inflow into a node can be confirmed within 18 s after the administration of Sonazoid. We accordingly determined that the minute blood flows were derived from the hepatic artery. Increased arterial flows were observed with the infiltration of chronic inflammatory cells of the histiocyte and lymphocyte types.

CEUS showed a contrast defect in the cystic areas and a delayed enhancement of the solid areas in the postvascular phase, which may reflect aggregation of siderophores. For example, in the case of echinococcosis, hepatobiliary cystadenoma/adenocarcinoma, cystic metastases, or CCC, CEUS shows contrast defects of the entire tumor in the postvascular phase (Table 2). Therefore, the two findings in CEUS (minute arterial flows into the tumor along the nodal septum in the vascular phase and contrast defects of the cystic areas and delayed enhancement of solid areas in the postvascular phase) are potentially useful for diagnosing an ancient schwannoma by recognizing the hemorrhage involved in the secondary degeneration and aggregation of siderophores.

The discrimination of a benign or a malignant schwannoma is difficult with preoperative imaging. However, some findings may indicate the presence of rare neoplasms such as a malignant schwannoma. The radiological features of hepatic malignant schwannoma include a well-demarcated, hypodense mass on CT, non-enhancement

on enhanced CT, and hypovascularity on angiography; in particular, hypovascularity may be an important finding for diagnosis, because most malignant hepatic tumors are hypervascular. Another important finding is the high level of alkaline phosphatase in serum with normal serum levels of hepatic transaminase and tumor markers, including CEA and AFP[13]. Nonetheless, because discrimination between a benign and malignant schwannoma is difficult, surgery is typically recommended.

In cases of malignant schwannoma, there are no reported chemotherapies and the prognosis is poor. Because the schwannoma may be tightly attached to Glisson's sheath (as in this case), surgical removal of the tumor could be very difficult, and hepatectomy that includes Glisson's sheath could be required.

In conclusion, here, we report a case of benign schwannoma, which we diagnosed using a novel method that combined CEUS with CT, MRI and PET. Because it is difficult to discriminate between a benign or malignant schwannoma of the liver, surgery is generally recommended for such tumors. Our findings with CEUS revealed minute arterial flow into the tumor along the nodal septum in the vascular phase, and delayed enhancement of solid areas in the postvascular phase. These two key observations may be useful in diagnosing an ancient schwannoma by recognizing the hemorrhage involved in the secondary degeneration and aggregation of siderophores.

REFERENCES

1 **Enzinger FM**, Weiss SW. Benign tumors of peripheral nerves. In: Soft Tissue Tumors. 5th ed. New York: Elsevier, 2008: 853-869

2 **Brennan MF**, Singer S, Maki RG, O'sullivan B. Soft tissue sarcoma. In: Cancer: Principles & Practice of Oncology. Philadelphia: Lippincott Williams & Wilkins, 2000: 1595

3 **Ozkan EE**, Guldur ME, Uzunkoy A. A case report of benign schwannoma of the liver. *Intern Med* 2010; **49**: 1533-1536

4 **Sukegawa R**, Matsumoto A, Suzuki S, Tominaga M, Koizumi K, Kikuchi Y, Ozawa K, Chiba A, Taruishi M, Hanawa M, Saitoh Y. [Primary diaphragmatic schwannoma which needed to be distinguished from a liver tumor]. *Nihon Shokakibyo Gakkai Zasshi* 2010; **107**: 93-101

5 **Shih YC**, Chen YL, Fang HY, Wu CY, Lin YC, Lin YM. Schwannoma mimicking liver tumor. *Thorac Cardiovasc Surg* 2009; **57**: 436-439

6 **Akin M**, Bozkirli B, Leventoglu S, Unal K, Kapucu LO, Akyurek N, Sare M. Liver schwannoma incidentally discovered in a patient with breast cancer. *Bratisl Lek Listy* 2009; **110**: 298-300

7 **Lee WH**, Kim TH, You SS, Choi SP, Min HJ, Kim HJ, Lee OJ, Ko GH. Benign schwannoma of the liver: a case report. *J Korean Med Sci* 2008; **23**: 727-730

8 **Momtahen AJ**, Akduman EI, Balci NC, Fattahi R, Havlioglu N. Liver schwannoma: findings on MRI. *Magn Reson Imaging* 2008; **26**: 1442-1445

9 **Flemming P**, Frerker M, Klempnauer J, Pichlmayr R. Benign schwannoma of the liver with cystic changes misinterpreted as hydatid disease. *Hepatogastroenterology* 1998; **45**: 1764-1766

10 **Wada Y**, Jimi A, Nakashima O, Kojiro M, Kurohiji T, Sai K. Schwannoma of the liver: report of two surgical cases. *Pathol Int* 1998; **48**: 611-617

11 **Fiel MI**, Schwartz M, Min AD, Sung MW, Thung SN. Malignant schwannoma of the liver in a patient without neurofibromatosis: a case report and review of the literature. *Arch Pathol Lab Med* 1996; **120**: 1145-1147

12 **Sheikh MY**, Husen YA, Pervez S, Khalid TR, Jaffer N, Afzal M. Computed tomography appearance of malignant schwannoma of the liver. *Can Assoc Radiol J* 1996; **47**: 183-185

13 **Morikawa Y**, Ishihara Y, Matsuura N, Miyamoto H, Kakudo K. Malignant schwannoma of the liver. *Dig Dis Sci* 1995; **40**: 1279-1282

14 **Yoshida M**, Nakashima Y, Tanaka A, Mori K, Yamaoka Y. Benign schwannoma of the liver: a case report. *Nihon Geka Hokan* 1994; **63**: 208-214

15 **Heffron TG**, Coventry S, Bedendo F, Baker A. Resection of primary schwannoma of the liver not associated with neurofibromatosis. *Arch Surg* 1993; **128**: 1396-1398

16 **Hytiroglou P**, Linton P, Klion F, Schwartz M, Miller C, Thung SN. Benign schwannoma of the liver. *Arch Pathol Lab Med* 1993; **117**: 216-218

17 **Abe S**, Miura Y, Matsukuma H, Taoka Y, Takeda N. [The difficulty of distinguishing retroperitoneal schwannoma from liver tumor in the caudate lobe]. *J UOEH* 1987; **9**: 411-416

18 **Tuder RM**, Moraes CF. Primary semimalignant Schwannoma of the liver. Light and electron microscopic studies. *Pathol Res Pract* 1984; **178**: 345-348

19 **Kim YC**, Park MS. Primary hepatic schwannoma mimicking malignancy on fluorine-18 2-fluoro-2-deoxy-D-glucose positron emission tomography-computed tomography. *Hepatology* 2010; **51**: 1080-1081

S- Editor Gou SX **L- Editor** Kerr C **E- Editor** Zhang DN